

## Analogies between granular jamming and the liquid-glass transition

Leonardo E. Silbert,<sup>1</sup> Deniz Ertaş,<sup>2</sup> Gary S. Grest,<sup>1</sup> Thomas C. Halsey,<sup>2</sup> and Dov Levine<sup>3</sup>

<sup>1</sup>Sandia National Laboratories, Albuquerque, New Mexico 87185

<sup>2</sup>Corporate Strategic Research, ExxonMobil Research and Engineering, Annandale, New Jersey 08801

<sup>3</sup>Department of Physics, Technion, Haifa 32000, Israel

(Received 5 September 2001; published 21 May 2002)

Based on large-scale, three-dimensional chute flow simulations of granular systems, we uncover strong analogies between the jamming of the grains and the liquid-glass transition. The angle of inclination  $\theta$  in the former transition appears as an analog of temperature  $T$  in the latter. The transition is manifested in the development of a plateau in the contact normal force distribution  $P(f)$  at small forces, the splitting of the second peak in the pair-correlation function  $g(r)$ , and increased fluctuations of the system energy. The static state also exhibits history dependence, akin to the quench-rate dependence of structural properties of glasses, due to the hyperstaticity of the contact network.

DOI: 10.1103/PhysRevE.65.051307

PACS number(s): 46.55.+d, 45.70.Cc, 46.25.-y, 64.70.Pf

Granular materials are many-body systems which can exhibit properties of both liquids and solids, often at the same time. Features such as jamming in silos and hoppers [1] and heterogeneous force propagation [2] have motivated proposals for constitutive relations for granular materials [3], in contrast to the established elastoplastic theories [4,5]. Moreover, the emerging field of “jammed systems” [6] seeks to understand whether analogies may be drawn between diverse systems which have the common properties that they are far from equilibrium, and unable to explore phase space.

O’Hern *et al.* [7] have recently shown that similarities exist between the properties of *static* granular packings and other amorphous systems; in particular, they compared force distributions for simulated systems of soft spheres undergoing a glass transition with experimental data from static granular packings [2,8]. These studies suggest that it may be interesting to consider the transition of granular materials from flowing to static, and inquire about its similarities with the glass transition [9,10].

In this article we study the dynamic jamming transition of systems of athermal grains through large-scale simulation. In particular, we consider the behavior of dense packings of granular particles flowing down a rough, inclined plane. We use the tilt angle  $\theta$  as the parameter that controls the transition from a flowing to a static state at the angle of repose  $\theta_r$ . Our earlier simulation studies in this geometry [11] have proven their reliability by reproducing key experimentally observed characteristics of dense granular flows [12].

The transition from flowing to static states as  $\theta$  is reduced below  $\theta_r$  has the following characteristics that are similar to a thermally driven glass transition.

(1)  $P(f)$ , the probability distribution of normal forces, develops a plateau in the static state.

(2)  $g(r)$ , the radial distribution function, indicates an amorphous structure which develops a split second peak near the transition.

(3) The contact networks of the static states are “hyperstatic” [13], i.e., the stresses inside the pile cannot be uniquely determined from loading conditions alone. The stresses start to depend on loading history as  $\theta$  is reduced

below  $\theta_r$ , reminiscent of the way a supercooled liquid falls out of equilibrium as it is cooled through the glass transition temperature  $T_g$ .

We also observe a discontinuous change in the number and nature of interparticle contacts: the fraction of contacts at Coulomb yield jumps from a finite value for flowing piles to zero for static piles [14]. This is accompanied by a jump in the average coordination number to well above four — four being the coordination number for an “isostatic” pile which has the minimal coordination required to satisfy force and torque balance on each frictional sphere [15,16]. We also find that the energy fluctuations of the system become  $O(1)$  in the vicinity of  $\theta_r$ .

We carried out molecular dynamics simulations in three-dimensions on a model system of  $N=8000$  monodisperse, cohesionless, frictional spheres of diameter  $d$  and mass  $m$ . The system is spatially periodic in the  $xy$  (flow-vorticity) plane, and is constrained by a rough bottom bed in the  $z$  direction, with a free top surface. The static packing height is about  $40d$ . Particles interact only on contact through a Hertzian interaction law in the normal and tangential directions to their lines of centers [17,18]. That is, contacting particles  $i$  and  $j$  positioned at  $\mathbf{r}_i$  and  $\mathbf{r}_j$  experience a relative normal compression  $\delta=|\mathbf{r}_{ij}-d|$ , where  $\mathbf{r}_{ij}=\mathbf{r}_i-\mathbf{r}_j$ , which results in a force  $\mathbf{F}_{ij}=\mathbf{F}_n+\mathbf{F}_t$ . The normal and tangential contact forces are given by

$$\mathbf{F}_n = \sqrt{\delta/d} \left( k_n \delta \mathbf{n}_{ij} - \frac{m}{2} \gamma_n \mathbf{v}_n \right), \quad (1)$$

$$\mathbf{F}_t = \sqrt{\delta/d} \left( -k_t \Delta \mathbf{s}_t - \frac{m}{2} \gamma_t \mathbf{v}_t \right), \quad (2)$$

where  $\mathbf{n}_{ij}=\mathbf{r}_{ij}/r_{ij}$ , with  $r_{ij}=|\mathbf{r}_{ij}|$ ,  $\mathbf{v}_n$  and  $\mathbf{v}_t$  are the normal and tangential components of the relative surface velocity, and  $k_{n,t}$  and  $\gamma_{n,t}$  are elastic and viscoelastic constants, respectively.  $\Delta \mathbf{s}_t$  is the elastic tangential displacement between spheres, obtained by integrating surface relative velocities during elastic deformation of the contact [19]. The magnitude of  $\Delta \mathbf{s}_t$  is truncated as necessary to satisfy a local Cou-

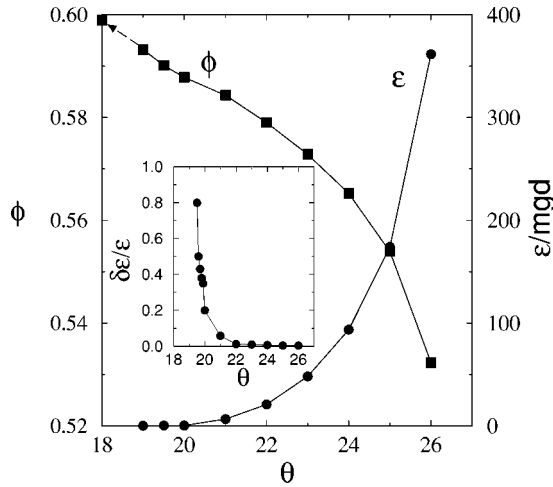


FIG. 1. Bulk packing fraction  $\phi$  and bulk averaged kinetic energy  $\epsilon$  per particle, normalized by  $mgd$ , as a function of tilt angle  $\theta$ . The dashed arrow indicates the value of  $\phi$  when  $\theta$  is reduced from  $19^\circ$  to  $0^\circ$ . Inset shows how the fluctuations in the energy  $\delta\epsilon$  become  $O(1)$  as the transition is approached.

lomb yield criterion  $F_t \leq \mu F_n$ , where  $F_t \equiv |\mathbf{F}_t|$  and  $F_n \equiv |\mathbf{F}_n|$ , and  $\mu$  is the local particle friction coefficient.

In the steady-state flow regime, changes in the particle friction  $\mu$ , the damping coefficients  $\gamma_{n,t}$ , or particle hardness  $k_n$ , do not change the qualitative nature of our findings [11]. For the present simulations we set  $k_n = 2 \times 10^5 mg/d$ ,  $k_t = \frac{2}{7} k_n$ ,  $\gamma_n = 50 \sqrt{g/d}$ ,  $\gamma_t = 0.0$ , and  $\mu = 0.5$  [20]. We choose a time step  $\delta t = 10^{-4} \tau$ , where  $\tau = \sqrt{d/g}$  and  $g$  is the gravitational acceleration.

To initiate flow, we tilt the bed to a large angle ( $\theta \approx 26^\circ$ ) long enough to remove any construction history. We then lower the angle, in unit increments, to the desired value in the range for which there is steady-state flow,  $20^\circ \leq \theta \leq 26^\circ$  [11]. In this range, the energy input from gravity is balanced by that dissipated in collisions.

In lowering  $\theta$ , the kinetic energy of the system decreases, though the fluctuations in the energy become large, see Fig. 1 inset. Flow continues to  $\theta_r (\approx 19.4^\circ$  for the set of parameters used here [21]). As shown in Fig. 1, the volume fraction  $\phi$ , increases as  $\theta$  is reduced. We generated further static packings by reducing the tilt from  $19^\circ$  to  $0^\circ$ . The volume fraction of the static packing for  $\theta = 0^\circ$ ,  $\phi = 0.599 \pm 0.005$ , is less than the random close packing value  $\phi_{rcp} \approx 0.64$ , for frictionless spheres [13].

We have investigated the distribution of contact forces in flowing and static states, by computing the probability density function (PDF)  $P(f)$ , where  $f \equiv F_n / \bar{F}_n(z)$  is the ratio of the normal contact force magnitude  $F_n$  to its average value at the depth  $z$  of each contact. Since our system is spatially periodic in the horizontal plane, with no side walls, the pressure does not saturate with depth, requiring separate averaging at each value of  $z$ . The data were averaged over 1000 configurations over a period of  $200\tau$  in the steady state at each flowing angle and 10 configurations for the static states.

As shown in Fig. 2, the PDFs for the flowing states exhibit exponential tails at high forces, whereas the static sys-

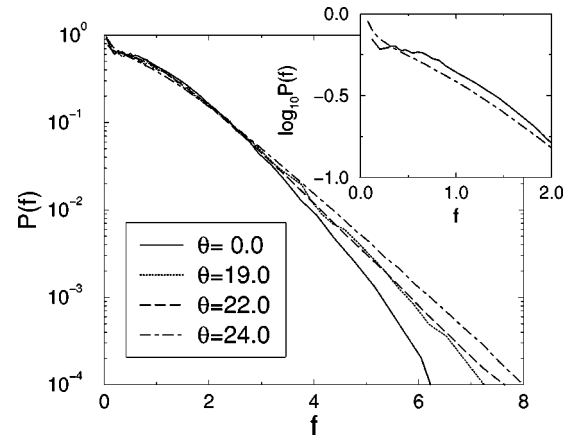


FIG. 2. Distribution of normal contact forces  $P(f)$  for various tilt angles (see text). The inset compares the data at  $24^\circ$  and  $0^\circ$ , showing the emergence of a plateau in  $P(f)$  at small forces in the jammed state.

tem appears more Gaussian [22]. When  $\theta$  is reduced below  $\theta_r$ , a plateau develops near  $f = 1$  (see inset), similar to the behavior observed in Ref. [7]. Upon further relaxation of the stress by reducing  $\theta$  to  $0^\circ$ , we obtain a PDF that is in quantitative agreement with experimental results from granular packings prepared differently [2,8]. Thus, the transition we observe appears to belong to the same family of jamming/glass transitions studied before [7].

We found subtle structural evidence for the transition from flow to rest, similar to what is observed in a supercooled liquid as one approaches the glass transition. We computed the radial distribution function (RDF)  $g(r)$ , shown in Fig. 3, to show changes in local structure as the system approaches the jammed state. Although the RDF is generally not isotropic for such sheared systems [23], this anisotropy is weak for the flowing states — peak positions do not shift as a function of angle. Thus, it is appropriate to consider an angularly averaged RDF to study the changes in short-range order. In the inset to Fig. 3 we observe the growth and gradual splitting of the second peak as  $\theta$  is reduced. The system becomes locally more structured as it compactifies

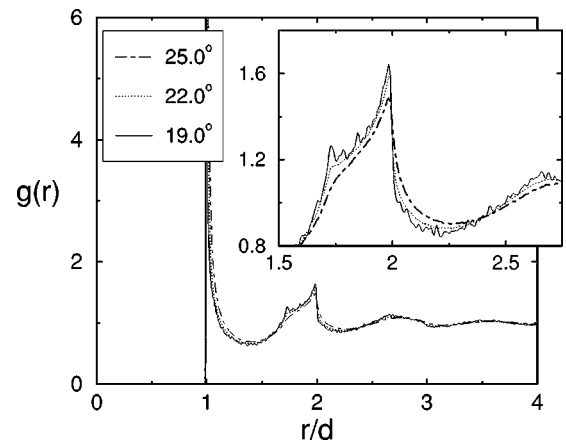


FIG. 3. Radial distribution function  $g(r)$  for various tilt angles  $\theta$ . The inset shows the region near the second peak.

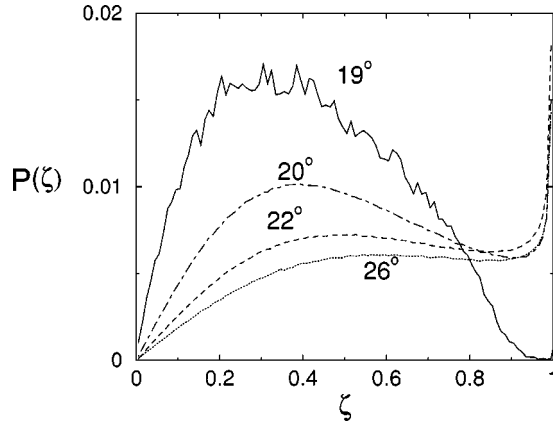


FIG. 4. The probability distribution  $P(\zeta)$  of frictional saturation  $\zeta \equiv F_t/\mu F_n$  at various tilt angles. In the flowing state a finite fraction of sliding contacts exist (see Fig. 5).

[24]. We see similar behavior for systems with small polydispersity.

An important characteristic that separates the granular system from a glass-forming liquid is the existence of interparticle friction and yield. To explore the influence of intergrain friction, we distinguish between intergrain frictional sliding contacts at their yield criterion  $F_t = \mu F_n$ , which respond plastically to some external perturbations, from contacts with  $F_t < \mu F_n$  (elastic contacts), whose response is determined by elastic deformations of the constituent grains.

We find that the nature of grain-grain contacts is quite different in the flowing and static regimes. The probability densities of frictional saturations  $\zeta \equiv F_t/\mu F_n$  are shown in Fig. 4 for various tilt angles. The fraction  $n_c$  of sliding contacts (with  $\zeta = 1$ ) decreases as the tilt angle is decreased towards  $\theta_r$  (see Fig. 5), accompanied by a decrease in the average frictional saturation of elastic contacts. For the static piles at  $\theta < \theta_r$ , almost all grain contacts are elastic.

A related question is whether or not static piles of rigid grains satisfy an isostaticity condition, where the number of

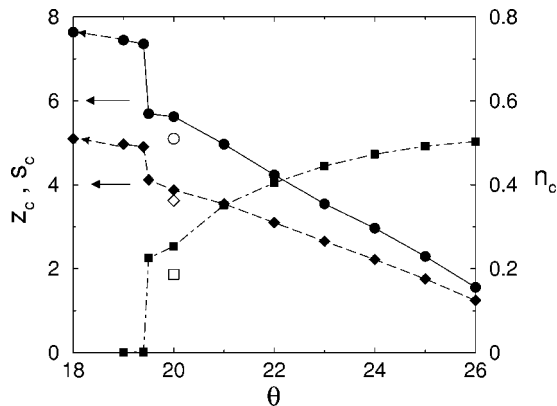


FIG. 5. As the tilt angle is decreased towards  $\theta_r$ , the fraction of sliding contacts  $n_c$  (squares) decreases while the coordination number  $z_c$  (diamonds) and the staticity index  $s_c$  (circles) increase. The isostatic values of  $z_c$  and  $s_c$  are indicated by the solid arrows. The dashed arrows indicate the values of  $z_c$  and  $s_c$  when we take  $\theta$  down to  $0^\circ$  from a stopped state. The open symbols at  $\theta = 20^\circ$  are for  $k_n = 2 \times 10^7 mg/d$ .

contacts is the minimum required to satisfy force and torque balance equations for each grain [15,16]. This isostaticity hypothesis has been frequently invoked in recent theoretical work attempting to derive macroscopic constitutive relations directly from the microstates of static granular packings [25]. Isostaticity is required for a unique determination of the individual contact forces solely in terms of the microstate. Otherwise, the details of grain deformations (for example, Hookean or Hertzian force laws) must be considered in order to determine the stress state of the pile [26], as the rigid grain problem becomes illposed.

Counting the degrees of freedom (DOF) in the contact forces suggests that isostaticity requires  $z_c = 4$  for frictional contacts (with three DOF—one vector force—per contact and six equations per grain) and  $z_c = 6$  for frictionless contacts (with one DOF—one normal force—per contact but only three equations per grain) for spherical grains. However, one DOF is eliminated for each frictional contact that reaches the yield criterion and becomes a sliding contact [26]: the magnitude of the tangential force in this case is determined by the normal force and the friction coefficient  $\mu$ . Thus, if the fraction of sliding contacts is  $n_c$ , for a coordination number  $z_c$  the total number of DOF characterizing interparticle forces is

$$N_f = \frac{N}{2} z_c [3(1 - n_c) + 2n_c], \quad (3)$$

and requiring  $N_f \geq 6N$  to match the number of kinematic constraints on the particles yields

$$s_c \equiv (3 - n_c) z_c / 2 \geq 6, \quad (4)$$

where we have defined the staticity index  $s_c$ . The equality corresponds to isostaticity. By analogy to the system in Ref. [26], the response of “hyperstatic” piles with  $s_c > 6$  to external forces cannot be determined without considering the history of grain contacts.

Figure 5 depicts  $s_c$  as a function of  $\theta$ . As expected,  $s_c < 6$  for all flowing piles, though it increases with decreasing  $\theta$ . However, it appears that a finite jump of  $s_c$  at  $\theta_r$  leaves the static pile significantly hyperstatic. The open symbols in Fig. 4 are for a system where  $k_n = 2 \times 10^7 mg/d$ , indicating that grain hardness is a relevant parameter in determining  $s_c$  and  $z_c$  [13].

What do these observations teach us about the nature of the “jamming” transition of the granular medium? Our earlier work showed that granular flows obey a local rheology independent of the history of loading [11]. Also, static piles are known to generally be able to support a range of external stresses without any macroscopic rearrangement, consistent with the existence of a hyperstatic contact network. So, how was the original stress state and associated configuration of grains in this static pile determined? One possible answer is that this state was determined by the local loading conditions at the instant the flow ceased. This is evidenced by different packing densities and coordination numbers achieved when the static system is prepared differently [13]. This resolution is akin to ideas discussed in the fixed principal axes (FPA)

model [3], except that the stress state of the static pile, including principal stress axes, do change subsequent to flow arrest (which is manifested as burial in the FPA model) as a function of external loading, due to contact elasticity of grains.

In summary, we have observed analogies between jamming of granular media driven by inclination angle  $\theta$  and the liquid-glass transition driven by temperature  $T$ . In particular, the evolution of the contact force distribution and the radial distribution function near the transition, at  $\theta_r$  and  $T_g$ , respectively, are very similar. Furthermore, the hyperstatic na-

ture of the static packings imply packing densities and stress states that are history dependent, analogous to the way the state of the glass at  $T < T_g$  depends on the quench rate. Finally, we note that we have performed a similar study with Hookean spheres, with essentially the same results.

Sandia is a multiprogram laboratory operated by Sandia Corporation, a Lockheed Martin Company, for the United States Department of Energy under Contract No. DE-AC04-94AL85000. D.L. acknowledges support from U.S.-Israel Binational Science Foundation through Grant No. 1999235.

- 
- [1] K. To, P.-Y. Lai, and H.K. Pak, Phys. Rev. Lett. **86**, 71 (2001).  
 [2] D.M. Mueth, H.M. Jaeger, and S.R. Nagel, Phys. Rev. E **57**, 3164 (1998).  
 [3] M.E. Cates, J.P. Wittmer, J.-P. Bouchaud, and P. Claudin, Phys. Rev. Lett. **81**, 1841 (1998); J.P. Wittmer, M.E. Cates, and P. Claudin, J. Phys. I **7**, 39 (1997).  
 [4] R. M. Nedderman, *Statics and Kinematics of Granular Materials* (Cambridge University, Cambridge, 1992).  
 [5] S.B. Savage, J. Fluid Mech. **377**, 1 (1998).  
 [6] A.J. Liu and S.R. Nagel, Nature (London) **396**, 21 (1998).  
 [7] C.S. O'Hern, S.A. Langer, A.J. Liu, and S.R. Nagel, Phys. Rev. Lett. **86**, 111 (2001).  
 [8] D.L. Blair, N.W. Mueggenburg, A.H. Marshall, H.M. Jaeger, and S.R. Nagel, Phys. Rev. E **63**, 041304 (2001).  
 [9] G. D'Anna and G. Grest, Phys. Rev. Lett. **87**, 254302 (2001).  
 [10] A. Barrat, J. Kurchan, V. Loreto, and M. Sellitto, Phys. Rev. E **63**, 051301 (2001).  
 [11] L.E. Silbert, D. Ertas, G.S. Grest, T.C. Halsey, D. Levine, and S.J. Plimpton, Phys. Rev. E **64**, 051302 (2001); D. Ertas, G.S. Grest, T.C. Halsey, D. Levine, and L.E. Silbert, Europhys. Lett. **56**, 214 (2001).  
 [12] O. Pouliquen, Phys. Fluids **11**, 542 (1999).  
 [13] L.E. Silbert, D. Ertas, G.S. Grest, T.C. Halsey, and D. Levine, Phys. Rev. E **65**, 031304 (2002).  
 [14] Using a sufficiently large value for interparticle friction, we did not see sliding contacts even in the flowing state.  
 [15] C.F. Moukarzel, Phys. Rev. Lett. **81**, 1634 (1998).  
 [16] J.-N. Roux, Phys. Rev. E **61**, 6802 (2000).  
 [17] O.R. Walton and R.L. Braun, J. Rheumatol. **30**, 949 (1986).  
 [18] P.A. Cundall and O.D.L. Strack, Geotechnique **29**, 47 (1979).  
 [19] We also take into account the rigid body motion around the contact point, ensuring that  $\Delta \mathbf{s}_i$  always remains in the local tangent plane of contact.  
 [20] Since the coefficient of restitution is dependent on  $\mathbf{v}_n$  and goes to 1 as  $\mathbf{v}_n \rightarrow 0$ , we increased the global damping for  $\theta < \theta_r$  after the measured kinetic energy per particle  $< 10^{-3} mgd$ . This was done to reduce the computer time needed to dissipate the remaining kinetic energy. In the static case the simulations were continued until the average kinetic energy per particle was less than  $10^{-8} mgd$ .  
 [21] In general, the specific value of  $\theta_r$  depends on  $\mu$  and  $\gamma_n$ , and is sensitive to roughness of the fixed bed.  
 [22] C.S. O'Hern, S.A. Langer, A.J. Liu, and S.R. Nagel, Phys. Rev. Lett. **88**, 075507 (2002).  
 [23] C.S. Campbell and C.E. Brennen, J. Fluid Mech. **151**, 167 (1985).  
 [24] A.S. Clarke and H. Jonsson, Phys. Rev. E **47**, 3975 (1993).  
 [25] S.F. Edwards and D.V. Grinev, Physica A **263**, 545 (1999).  
 [26] T.C. Halsey and D. Ertas, Phys. Rev. Lett. **83**, 5007 (1999).